



Three-dimensional modeling of heat transfer during freezing of suspended and in-contact-with-a-surface yellow potatoes and ullucus

WALTER SALAS-VALERIO^{1,2} | MIGUEL SOLANO-CORNEJO^{2,3} |

MOISÉS ZELADA-BAZÁN² | JULIO VIDAURRE-RUIZ^{2,3}

Publicado: 13/08/2021 | Ed.1, 2021

Abstract

The aim of this research was to model the heat transfer during the freezing process of cubed yellow potatoes (*Solanum tuberosum* L.) and ullucus (*Ullucus tuberosus* Caldas). A mathematical model was developed using the three-dimensional (3D) finite difference scheme to simulate the freezing process of suspended and in-contact-with-a-surface cubic particles. The thermophysical properties were predicted using the proximal composition and the convective heat transfer coefficient (h) was obtained by optimizing the root mean square error (RMSE) value. A pseudo h was included to simulate the heat transfer of cubic particles in-contact-with-a-surface. Low values of h were found for suspended frozen cubes (17–27 W/m²C) and high values of pseudo h (295–371 W/m²C) were determined for frozen cubes in-contact-with-a-surface. An excellent agreement was observed between experimental and predicted temperatures histories (RMSE: 0.6–1.7°C) at different

thermocouples positions. In conclusion, the developed model simulated correctly the freezing profile of potato and ullucu in cubic shape. With this model, the possible effects of h and external temperature on freezing times of these vegetables under different positions were evaluated and were represented by polynomial equations that could be used in the industry.

Practical Applications

In this research, a simple and easy-to-implement mathematical model was developed to simulate the heat transfer during freezing process of yellow potatoes and ullucus in cubes. The 3D finite difference scheme developed can be used to simulate the freezing of suspended cubed food, as is the case of fluidized bed freezers, or that are in contact with a metal surface, as in plate freezers. In addition, this study presented polynomial equations that allow the quick and precise calculation of the freezing times of cubed yellow potatoes and ullucus.

¹Faculty of Food Industry Engineering, Department of Food Engineering, National Agrarian University, La Molina, Peru

²Research Group Food Engineering, National Agrarian University, La Molina, Peru

³Faculty of Engineering, Architecture and Urbanism, Department of Industrial Engineering, Señor de Sipán University, Lambayeque, Peru

Correspondence

Walter Salas-Valerio, Faculty of Food Industry Engineering, Department of Food Engineering, National Agrarian University, La Molina, Lima 12, Peru.

Email: wfsalas@lamolina.edu.pe

1 | INTRODUCTION

The freezing process is the reducing of the temperature of food below its freezing point (James, Purnell, & James, 2015). Freezing is used for preserving food because it decreases the speed of physical, chemical, and sensory reactions (Wu, Zhang, Adhikari, & Sun, 2017; Xu, Zhang, Mujumdar, & Adhikari, 2017). Peru is a large exporter of fruits and vegetables, being the United States one of its most important markets (Meade, Baldwin, & Calvin, 2010). Peruvian frozen vegetables are highly valued in market due to their nutritional and functional components. Some of them are potatoes (*Solanum tuberosum* L.), ullucus (*Ullucus tuberosus* Caldas), mashuas (*Tropaeolum tuberosum* Ruiz & Pavón), and ocas (*Oxalis tuberosa* Molina) which are Andean tubers that have been widely investigated on its nutritional and functional properties (Campos et al., 2006; Campos, Chirinos, Gálvez Ranilla, & Pedreschi, 2018).

The commercial way to freeze vegetables in Peru is using a freezer plate or an IQF fluidized bed freezer where the vegetables are first cut into regular shapes to reduce their size. Then they are subjected to the blanching process and cooled quickly.

The correct mathematical modeling of heat transfer during food freezing is necessary to design and optimize the freezing process. The mathematical modeling of heat transfer in food freezing is a special challenge (Pham, 2006) because the freezing process is a nonlinear heat conduction phenomenon (Dima, Santos, Baron, Califano, & Zartzyk, 2014; Wang et al., 2007). Two mathematical methods can be employed to determinate the freezing time. One of them is the analytical model. This model is the modification and extension of the Plank equation (López-Leiva & Hallström, 2003), which shows problems due to unrealistic assumptions that are considered. The other one is the numerical method where it is possible to estimate the changes in temperature as a function of the physical characteristics of the food and its enthalpy change (Delgado & Sun, 2001). The advantage of numerical methods over simple equations is that effects of the phase change over a range of temperature, changing thermal properties, and heterogeneity of food products can be analyzed. Thus, numerical methods are good methods to analyze food freezing (Delgado & Sun, 2001; Dima et al., 2014; Wang et al., 2007). There are several numerical solutions to simulate heat transfer during freezing. Among the most used methods for food processing are finite difference method (FDM), finite element method, and finite volume method (Delgado & Sun, 2001; Pham, 2006; Zhao & Takhar, 2017).

The FDM has been widely used to simulate the heat transfer during freezing of foods because it is easy to program and it is useful when it comes to almost perfectly in regular shapes (Delgado & Sun, 2001; Pham, 2006). Even some recent research used the FDM to discretized the equations proposed in the

method of lines to predict the freezing times for cylinders, spheres, and slab (Ferreira, 2017; Ferreira, Rojas, Souza, & Oliveira, 2016).

The first works reported in literature date back to 40 years ago. Cleland and Earle (1977, 1979), Cleland, Cleland, and Earle (1987), and Loeffen, Earle, and Cleland (1981) present different finite difference schemes to simulate heat transfer during freezing of slab, cylinders, spherical, and rectangular brick foodstuff based on temperature methods with temperature as the only dependent variable. Mannapperuma and Singh (1988) developed an explicit FDM, involving enthalpy formulation to predict temperature distribution during freezing of slabs, cylinders, spheres, two-, and three-dimensional (3D) shapes. Pham (1985) proposed a FDM that combines enthalpy and temperature methods. The method was validated with experimental data of one dimension (1D). Tocci and Mascheroni (1995) developed two explicit FDMs to simulate simultaneous heat and mass transfer during freezing of meat balls. One scheme proposed was with constant mesh size, and the other was with equal volume elements. The authors reported that there were no significant differences between the results obtained with both numerical schemes tested. Saad and Scott (1997) evaluated the accuracy of two FDMs, comparing with an analytical solution and experimental data of codfish freezing (1D). The researchers conclude that the two-step FDM presented better accuracy than the Crank-Nicolson method. Wang et al. (2007) developed a 1D FDM using Crank-Nicolson scheme to simulate the freezing time of individual food. The method showed good results with reported freezing times of slice, cylindrical, and spherical foodstuffs. Norton, Delgado, Hogan, Grace, and Sun (2009) developed a 1D FDM based on the enthalpy method to simulate high pressure freezing of tylose, agar gel, and potatoes. This model is able to estimate the freezing time profile considering the shifting effect of pressure on the enthalpy curve, the initial freezing temperature, and the thermophysical properties of the food.

All the above-mentioned research used a convective heat transfer coefficient in general (h), without considering that h depends on many factors such as the direction of heat flow. This parameter is necessary for designing the freezing process and has also been found to be a major source of error in modeling the freezing process (Ebrahimnia-Bajestan, Niazmand, Etminan-Farooji, & Ebrahimnia, 2012). Only a few studies consider the influence of different heat transfer coefficients related to the position of the food in the freezing system (Dima et al., 2014; Ebrahimnia-Bajestan et al., 2012). Therefore, the aim of this research was to develop a 3D model to simulate the heat transfer during freezing process of suspended and in-contact-with-a-surface food, including different h values according to the position of the food in the freezing system.

2 | MATERIALS AND METHOD

2.1. | Conditioning of the raw material and freezing process

In order to validate the mathematical model proposed, yellow potatoes (*S. tuberosum* L.), ullucus (*U. tuberosus* Caldas), and a model food system (agar gel 2%) were used. These two vegetables were selected because they are Peruvian foods with export potential to the American and European markets and the agar gel was selected because its composition is 99% water, and according to Norton et al. (2009), its thermal properties are known and could avoid the calculation error in the simulation.

The composition of potato and ullucu was determined in triplicate using Association of Official Analytical Chemists (2000) methods. The raw materials were washed, peeled and cut into cubes of 2 × 2 × 2 cm for yellow potatoes and 1.5 × 1.5 × 1.5 cm for ullucus.

The freezing process was performed in a tunnel freezer, something similar to industrial conditions can be obtained using this type of tunnel with cold air. Two thermocouples (Type K) were placed in the cubes (potatoes, ullucus, and agar gel), one at the center and one on the surface. The air temperature was -25°C and the residence time was 50 min. The cubic particles were frozen in two positions. The first was suspended and the other supported on the surface of the freezer. The temperature was recorded every second with a multimeter connected to a personal computer. The accuracy of the equipment was of ±2°C. All freezing experiments were conducted in triplicate.

2.2. | Thermophysical properties of frozen and unfrozen foods

The initial freezing temperature (T_f) of potato and ullucu was determined using the equation proposed by Boonsupthip, Sajjaanantakul, and Heldman (2009) (Equation 1).

$$\frac{1}{T_f} = \frac{1}{T_{fo}} - \frac{RM_w}{\lambda} \ln \left[\frac{(X_u - X_b)/M_w}{(X_u - X_b)/M_w + \sum_i \left(\frac{X_i}{M_i} \right)} \right],$$

where the unfrozen water mass (X_u) during the freezing process was considered using mass fractions and molecular weights of specific food components such as proteins, carbohydrates, minerals, and acids/bases; T_{fo} is the melting point of water (273.15 K); R is the ideal gas constant (8.314 kJ/kg mol K); M_w is the molecular weight of water (18.02 g/mol); λ is the mass enthalpy change for fusion or the latent heat of fusion for water (333.64 kJ/kg); X_i and M_i are mass and molecular weight of the dry solid components with significant impact on the initial freezing temperature of the food (Boonsupthip et al., 2009). According to Boonsupthip and Heldman (2007) and Boonsupthip et al. (2009), the key composition data needed in the equation are the solutes contributing molalities at or above 50 μmol/100 g food like low-molecular weight carbohydrates, minerals, and acids/bases.

The bound water (X_b), defined as water that does not freeze at -40°C, was calculated using an empirical model proposed by Schwartzberg (1976) (Equation 2).

$$X_b = a X_s,$$

where a is an experimental coefficient factor defined for specific types of food products and X_s is the summation of dry solid mass fractions of proteins, carbohydrates, lipids, ashes, and fibers. According to Schwartzberg (1976), the value of a vegetable is between 0.25 and 0.18; for practical purposes, in this research, the value of 0.18 was used for both vegetables.

Thermophysical properties such as thermal conductivity, specific heat, and density were calculated for frozen and unfrozen foods based on the composition according to Choi and Okos (1986) (Equation 3). Table 1 shows the full polynomial equations developed by Choi and

TABLE 1 Thermal property equations for food components developed by Choi and Okos (1986)

Thermal property	Food component	Thermal property model
Thermal conductivity (W/m°C)	Protein	$k = 0.17881 + 1.1058 \times 10^{-3} T - 2.7178 \times 10^{-6} T^2$
	Lipids	$k = 0.18071 - 2.7604 \times 10^{-4} T - 1.7749 \times 10^{-7} T^2$
	Carbohydrate	$k = 0.20141 + 1.3874 \times 10^{-3} T - 4.3312 \times 10^{-6} T^2$
	Fiber	$k = 0.18331 + 1.2497 \times 10^{-3} T - 3.1683 \times 10^{-6} T^2$
	Ash	$k = 0.32962 + 1.4011 \times 10^{-3} T - 2.9069 \times 10^{-6} T^2$
	Water	$k = 0.57109 + 1.7625 \times 10^{-3} T - 6.7063 \times 10^{-6} T^2$
	Ice	$k = 2.2196 - 6.2459 \times 10^{-3} T + 1.0154 \times 10^{-4} T^2$
Density (kg/m ³)	Protein	$\rho = 1.3299 \times 10^3 - 5.1840 \times 10^{-1} T$
	Lipids	$\rho = 9.2559 \times 10^2 - 4.1757 \times 10^{-1} T$
	Carbohydrate	$\rho = 1.5991 \times 10^3 - 3.1046 \times 10^{-1} T$
	Fiber	$\rho = 1.3115 \times 10^3 - 3.6589 \times 10^{-1} T$
	Ash	$\rho = 2.4238 \times 10^3 - 2.8963 \times 10^{-1} T$
	Water	$\rho = 9.9718 \times 10^2 + 3.1439 \times 10^{-3} T - 3.7574 \times 10^{-3} T^2$
	Ice	$\rho = 9.1689 \times 10^2 - 1.3071 \times 10^{-1} T$
Specific heat (J/kg°C)	Protein	$c_p = 2.0082 \times 10^3 + 1.2089 T - 1.2129 \times 10^{-3} T^2$
	Lipids	$c_p = 1.9842 \times 10^3 + 1.4733 T - 4.8008 \times 10^{-3} T^2$
	Carbohydrate	$c_p = 1.5488 \times 10^3 + 1.9625 T - 5.9399 \times 10^{-3} T^2$
	Fiber	$c_p = 1.8459 \times 10^3 + 1.8306 T - 4.6509 \times 10^{-3} T^2$
	Ash	$c_p = 1.0926 \times 10^3 + 1.8896 T - 3.6817 \times 10^{-3} T^2$
	Water (0 to 150°C)	$c_p = 4.1762 \times 10^3 - 9.0864 \times 10^{-2} T + 5.4731 \times 10^{-3} T^2$
	Water (-40 to 0°C)	$c_p = 4.0817 \times 10^3 - 5.3062 T + 9.9516 \times 10^{-1} T^2$
Ice	$c_p = 2.0623 \times 10^3 + 6.0769 T$	

Note: T is the food temperature.

Okos (1986). As the model food system contains a high amount of water (99%), the thermophysical properties of water in liquid and solid state were used for the validation (Norton et al., 2009).

$$k = \sum_{i=1}^n k_i \frac{X_i/\rho_i}{\sum_{i=1}^n X_i/\rho_i} c_p = \sum_{i=1}^n c_{pi} X_i \rho_i = \frac{1}{\sum_{i=1}^n X_i/\rho_i},$$

where k is the thermal conductivity, c_p is the effective specific heat, and ρ is the density of the food.

Once the thermophysical properties have been determined, the variation of thermal conductivity and the apparent specific heat during freezing were calculated using Equations (4) and (5) developed by Schwartzberg (1977). They were then introduced in the finite difference scheme proposed. Only the food density was considered constant for temperatures below and above the initial freezing temperature

$$\begin{cases} k = k_f + (k_u - k_f) \left(\frac{T_{fo} - T_f}{T_{fo} - T} \right), & T \leq T_f, \\ k = k_u, & T > T_f, \end{cases}$$

$$\begin{cases} c_p = c_{pf} + (X_w - X_b X_s) \frac{\lambda (T_{fo} - T_f)}{(T_{fo} - T)^2}, & T \leq T_f, \\ c_p = c_{pu}, & T > T_f, \end{cases}$$

where k_f and k_u are the frozen and unfrozen thermal conductivity, respectively. Similarly, c_{pf} and c_{pu} are the frozen and unfrozen effective specific heat..

2.3. | Modeling heat transfer using 3D finite difference method

The mathematical model used to predict the freezing process of samples is based on Fourier's law and Fick's second law to calculate the unsteady 3D temperature inside the food in rectangular coordinates (x , y , and z) with temperature-dependent thermophysical food properties. The model is also based on certain assumptions related to the boundary conditions. The borders in contact with air had the same boundary conditions ($h1x = h1y = h1z$), while the border in-contact-with-a-surface was under another boundary condition ($h2x = h2z$). Under these assumptions, the mathematical model for the unsteady

3D freezing process is

$$\rho(T)c_p(T) \frac{\partial T}{\partial t} = \frac{\partial}{\partial x} \left(k(T) \frac{\partial T}{\partial x} \right) + \frac{\partial}{\partial y} \left(k(T) \frac{\partial T}{\partial y} \right) + \frac{\partial}{\partial z} \left(k(T) \frac{\partial T}{\partial z} \right).$$

The initial and boundary conditions are

$$\begin{aligned} T_x = T_y = T_z = T_i, & t = 0, \\ -k \frac{\partial T}{\partial x} \Big|_{L=x} &= h_{1x} [T_{\infty} - T_{(x=L)}], & t > 0, & \frac{L}{2} < x < L, \end{aligned}$$

$$-k \frac{\partial T}{\partial y} \Big|_{L=y} = h_{1y} [T_{\infty} - T_{(y=L)}], t > 0, \frac{L}{2} < y < L,$$

$$-k \frac{\partial T}{\partial z} \Big|_{L=z} = h_{1z} [T_{\infty} - T_{(z=L)}], t > 0, \frac{L}{2} < z < L,$$

$$-k \frac{\partial T}{\partial x} \Big|_{L=x} = h_{2x} [T_{\infty} - T_{(x=L)}], t > 0, 0 < x < \frac{L}{2},$$

$$-k \frac{\partial T}{\partial z} \Big|_{L=z} = h_{2z} [T_{\infty} - T_{(z=L)}], t > 0, 0 < x < \frac{L}{2}.$$

The numerical modeling of heat transfer was performed only for 1/4 of the whole cube volume (shaded volume in Figure 1), as thermal symmetry about the geometric center of particle exists due to the same boundary conditions at all surfaces for the case of the suspended cube ($h_{1x} = h_{1y} = h_{1z}$). In the same way, the modeling was performed for the cube in contact with the surface but considering pseudo boundary conditions ($h_{2x} = h_{2z}$).

An explicit finite difference scheme was used to solve Equations (6) and (7) for cubed food products. The scheme developed was written in programming language Visual Basic 2015 (Microsoft Corporation) using energy balance

method. Total of 7 nodes in the x-axis, 13 nodes in the y-axis, and 7 nodes in the z-axis were used for a cubic particle, with a time step of 0.125 s. Four types of nodes were programmed: one type of internal node and three types of external nodes. The internal nodes were connected with six nodes and the external nodes were connected with five, four, and three nodes, as appropriate. A similar proposal was developed by the authors to stimulate the blanching process of cubic particle (Vidaurre-Ruiz & Salas-Valerio, 2017).

The temperature for each time step for internal nodes, $T_{i,j,k}$, was calculated as follows:

$$\frac{T_{i,j,k}^{t+1} - T_{i,j,k}^t}{\Delta t} = \frac{k(T)}{\rho(T)c_p(T)} \left(\frac{T_{i+1,j,k}^t - 2T_{i,j,k}^t + T_{i-1,j,k}^t}{\Delta x^2} + \frac{T_{i,j+1,k}^t - 2T_{i,j,k}^t + T_{i,j-1,k}^t}{\Delta y^2} + \frac{T_{i,j,k+1}^t - 2T_{i,j,k}^t + T_{i,j,k-1}^t}{\Delta z^2} \right), \quad (8)$$

$$T_{i,j,k}^{t+1} = (1 - F_1 - F_2 - F_3 - F_4 - F_5 - F_6) T_{i,j,k}^t + F_1 (T_{i+1,j,k}^t) + F_2 (T_{i-1,j,k}^t) + F_3 (T_{i,j+1,k}^t) + F_4 (T_{i,j-1,k}^t) + F_5 (T_{i,j,k+1}^t) + F_6 (T_{i,j,k-1}^t), \quad (9)$$

where

$$F_1 = \frac{k_{i+1/2} \Delta t}{\rho c_p \Delta x^2}; F_2 = \frac{k_{i-1/2} \Delta t}{\rho c_p \Delta x^2}; F_3 = \frac{k_{j+1/2} \Delta t}{\rho c_p \Delta y^2}; F_4 = \frac{k_{j-1/2} \Delta t}{\rho c_p \Delta y^2}; F_5 = \frac{k_{k+1/2} \Delta t}{\rho c_p \Delta z^2}; F_6 = \frac{k_{k-1/2} \Delta t}{\rho c_p \Delta z^2}.$$

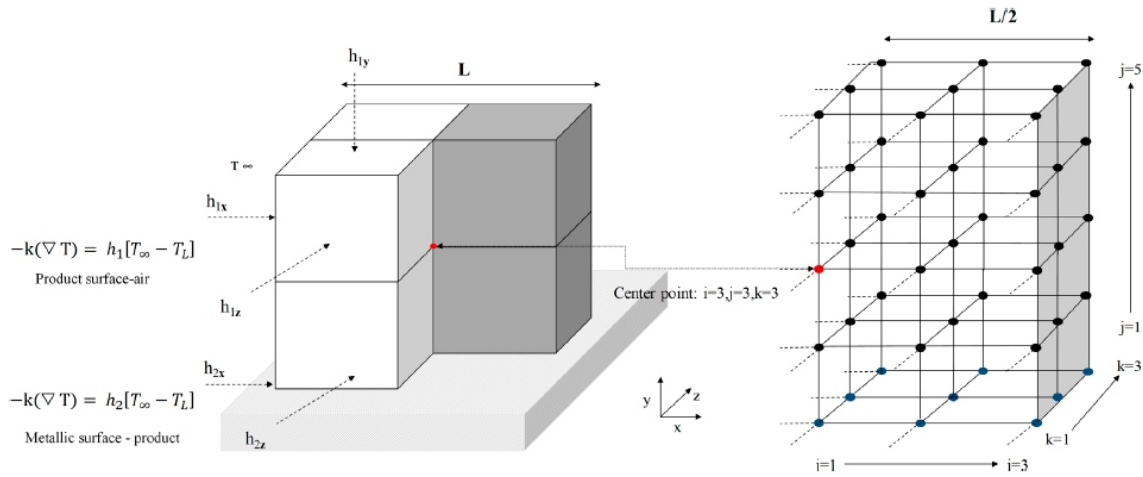


FIGURE1 An example of node generation for a mesh of 3 × 5 × 3 of a cubic particle in-contact-with-a-surface

$$k_{i+1/2} = \frac{T_{i,j,k}^t - T_{i+1,j,k}^t}{2}; k_{i-1/2} = \frac{T_{i,j,k}^t - T_{i-1,j,k}^t}{2};$$

$$k_{j+1/2} = \frac{T_{i,j,k}^t - T_{i,j+1,k}^t}{2}; k_{j-1/2} = \frac{T_{i,j,k}^t - T_{i,j-1,k}^t}{2};$$

$$k_{k+1/2} = \frac{T_{i,j,k}^t - T_{i,j,k+1}^t}{2}; k_{k-1/2} = \frac{T_{i,j,k}^t - T_{i,j,k-1}^t}{2}.$$

The temperature for each time step for external nodes, with five connections, $T_{i,j,k}^{t+1}$, was calculated as follows:

$$\rho c_p V_1 \frac{T_{i,j,k}^{t+1} - T_{i,j,k}^t}{\Delta t} = hA_1 (T_\infty - T_{i,j,z}^t) + kA_1 \frac{T_{i+1,j,k}^t - T_{i,j,k}^t}{\Delta x}$$

$$+ kA_1 \frac{T_{i-1,j,k}^t - T_{i,j,k}^t}{\Delta x} + kA_1 \frac{T_{i,j+1,k}^t - T_{i,j,k}^t}{\Delta y}$$

$$+ kA_1 \frac{T_{i,j-1,k}^t - T_{i,j,k}^t}{\Delta y} + kA_1 \frac{T_{i,j,k-1}^t - T_{i,j,k}^t}{\Delta z},$$

$$T_{i,j,k}^{t+1} = (1 - F7N_{Bi} - 4F7 - F8)T_{i,j,k}^t + F7N_{Bi}(T_\infty)$$

$$+ F7(T_{i+1,j,k}^t + T_{i-1,j,k}^t + T_{i,j+1,k}^t + T_{i,j-1,k}^t) + F8(T_{i,j,k-1}^t),$$

Where

$$F7 = \frac{\alpha \Delta t}{\Delta x^2/2}, F8 = \frac{k_{k-1/2} \Delta t}{\rho c_p \Delta z^2/2}, \text{ and } N_{Bi} = \frac{\Delta x h}{k},$$

considering that $\Delta x = \Delta y = \Delta z$.

And

$$k_{k-1/2} = \frac{T_{i,j,k}^t - T_{i,j,k-1}^t}{2}.$$

The temperature for each time step for external nodes, with four connections, $T_{i,j,k}^{t+1}$, was calculated as follows:

$$\rho c_p V_2 \frac{T_{i,j,k}^{t+1} - T_{i,j,k}^t}{\Delta t} = 2(hA_2 (T_\infty - T_{i,j,z}^t)) + kA_2 \frac{T_{i-1,j,k}^t - T_{i,j,k}^t}{\Delta x}$$

$$+ kA_2 \frac{T_{i+1,j,k}^t - T_{i,j,k}^t}{\Delta x} + kA_2 \frac{T_{i,j-1,k}^t - T_{i,j,k}^t}{\Delta y} + kA_2 \frac{T_{i,j,k-1}^t - T_{i,j,k}^t}{\Delta z},$$

where $F9 = \frac{\alpha \Delta t}{\Delta x^2/2}$ and $N_{Bi} = \frac{\Delta x h}{k}$, considering that $\Delta x = \Delta y = \Delta z$.

The temperature for each time step for external nodes, with three connections, $T_{i,j,k}^{t+1}$ was calculated as follows:

$$\rho c_p V_3 \frac{T_{i,j,k}^{t+1} - T_{i,j,k}^t}{\Delta t} = 3(hA_3 (T_\infty - T_{i,j,z}^t)) + kA_3 \frac{T_{i-1,j,k}^t - T_{i,j,k}^t}{\Delta x}$$

$$+ kA_3 \frac{T_{i+1,j,k}^t - T_{i,j,k}^t}{\Delta x} + kA_3 \frac{T_{i,j,k-1}^t - T_{i,j,k}^t}{\Delta z},$$

$$T_{i,j,k}^{t+1} = (1 - 3F10N_{Bi} - 3F10)T_{i,j,k}^t + 3F10N_{Bi}(T_\infty)$$

$$+ F10(T_{i-1,j,k}^t + T_{i+1,j,k}^t + T_{i,j,k-1}^t),$$

where $F10 = \frac{\alpha \Delta t}{\Delta x^2/2}$ and $N_{Bi} = \frac{\Delta x h}{k}$, considering that $\Delta x = \Delta y = \Delta z$.

In all cases, for $T_{i,j,k}^{t+1} \leq T_f$, k is obtained by substitution of temperature in Equation (4) an C_p is obtained by substitution of temperature in Equation (5). For $T_{i,j,k}^{t+1} \geq T_f$, $k = k_u$ and $c_p = c_{pu}$.

2.4. | Estimation of the convective heat transfer coefficient (h)

The convective heat transfer coefficient for suspended ($h1x = h1y = h1z$) and in-contact-with-a-surface ($h1x = h1y = h1z$ and $h2x = h2z$) cubed food were estimated by optimization of the root mean squares error (RMSE) of the experimental and predicted time-temperatures data (Equation 16).

Different freezing curves were simulated using the thermophysical properties previously calculated for each sample (Table 3), the external temperature (T_m) of -25°C , and different h values. For the case of the suspended cube, the $h1$ values ($h1x = h1y = h1z$) were tested in the range of 15–25 $\text{W/m}^2\text{C}$, and for the case of the cube in-contact-with-a-surface, the value of $h1$ ($h1x = h1y = h1z$) were tested in the range of 15–25 $\text{W/m}^2\text{C}$ and $h2$ ($h2x = h2z$) from 250 to 350 $\text{W/m}^2\text{C}$; in this case, the central composite design was used, in order to obtain simultaneously the optimal values of $h1$ and $h2$. The statistical analysis was performed with Statgraphics Centurion XVI software (Statpoint Technologies, Inc., Warrenton, VA).

$$\text{RMSE} = \sqrt{\frac{1}{n} \sum_{i=1}^n (T - T_{\text{simulation}})^2}.$$

3. | RESULTS AND DISCUSSION

3.1. | Composition and thermophysical properties of raw materials

Potatoes and ullucus are tubers with high contents of water (Table 2). Therefore, some thermal properties were very similar to the thermal properties of water. The composition of potatoes and ullucus were different in the content of monosaccharides, disaccharides, and minerals. According to Boonsupthip et al. (2009), these components are important in the prediction of the used model. The initial freezing temperature of the potato was lower than the ulluco (Table 3). Similar values were reported by Rahman, Machado-Velasco, Sosa-Morales, and Velez-Ruiz (2009). As for ullucus, up to now, there had not been values reported in literature.

As it was expected, the other thermophysical properties like density and specific heat decreased when the food was frozen, while the thermal conductivity increased almost four times due to the high water content in the food matrix (Table 3).

3.2. | Mathematical model validation

The best fit between simulation and experimental data of suspended cubed yellow potatoes was achieved using $17 \text{ W/m}^2\text{C}$. The RMSE

TABLE 2 Proximal composition of potato and ullucu per 100 g

Component	Potatoes	Ullucus
Water	77.90 ± 0.87	83.70 ± 1.01
Protein	2.40 ± 0.01	1.10 ± 0.03
Lipids	1.10 ± 0.03	0.10 ± 0.01
Total carbohydrates	15.45 ± 0.02	14.30 ± 0.03
Monosaccharides	1.30 ± 0.01	0.04 ± 0.01
Disaccharides	3.00 ± 0.02	0.01 ± 0.00
Fiber	2.70 ± 0.01	0.80 ± 0.02
Minerals	0.55 ± 0.01	0.80 ± 0.03
Acids/bases	0.74 ± 0.01	0.63 ± 0.02

was $2.2 \pm 1^\circ\text{C}$ for the center point and $1.6 \pm 0.5^\circ\text{C}$ for the external point (Figure 2).

For suspended cubed ullucus, the best fit was achieved using $19 \text{ W/m}^2\text{C}$ and the minimum value of RMSE was $0.59 \pm 0.2^\circ\text{C}$ for the center point. For in-contact-with-a-surface cubed ullucus, the best fit was achieved using $20.4 \text{ W/m}^2\text{C}$ for $h_{1x} = h_{1y} = h_{1z}$ and $294.9 \text{ W/m}^2\text{C}$ for $h_{2x} = h_{2z}$. The minimum value of RMSE was around of $1.3 \pm 0.2^\circ\text{C}$ for both types of cubes (Figure 3).

Similar values were determined for suspended cubes of agar gel. The best fit was achieved using $22 \text{ W/m}^2\text{C}$ and for $h_{1x} = h_{1y} = h_{1z}$. The minimum value of RMSE was $1.7 \pm 0.3^\circ\text{C}$ for the center point. For in-contact-with-a-surface cubes of agar gel, the best fit was achieved using $27 \text{ W/m}^2\text{C}$ for $h_{1x} = h_{1y} = h_{1z}$ and $370.7 \text{ W/m}^2\text{C}$ for $h_{2x} = h_{2z}$. The minimum value of RMSE was around of $1.2 \pm 0.4^\circ\text{C}$ for both types of cubes (Figure 4).

A good agreement between experimental and predicted values of temperature is shown using the numerical model for suspended and incontact-with-a-surface cubic particles. Few studies consider that there is a contact heat transfer coefficient. Dima et al. (2014) proposed a mathematical model to simulate the freezing process of crab meat packaged in pouches and crab claws. The authors considered two heat transfer coefficients, determined in an industrial tunnel freezer. The h values for pouches were h_1 (product-air) = $10 \text{ W/m}^2\text{C}$ and h_2 (belt-product) = $50 \text{ W/m}^2\text{C}$, and for crab

claws the h values were $h_1 = 20$ and $h_2 = 500 \text{ W/m}^2\text{C}$. Although h depends on many factors and is a difficult parameter to calculate directly (Fricke & Becker, 2006), it is necessary to achieve a good prediction in the simulation. Like the thermophysical properties, these parameters are tedious and complex to determinate directly from foods in the freezing temperature range (Cornejo, Cornejo, Ramirez, Almonacid, & Simpson, 2016). However, the procedure proposed in this work can be used to determine the thermophysical properties of the heat transfer properties of tubers with good precision and useful for the simulation of the freezing process.

3.3. | Equations to evaluate the effects of h and external temperature on freezing times

In order to develop equations that simplify the prediction of the freezing time of cubes, freezing profiles were simulated under different operating conditions varying the air temperature and h ($h_{1x} = h_{1y} = h_{1z}$), which depends to a large extent on the speed of the air.

Tables 4 and 5 show the freezing times need for the center point in cubed yellow potatoes and ullucus to reach a final value of -15°C , being the initial temperature of the cubes 20°C and considering different external temperatures and heat transfer coefficients at the interface product air. For the case of cubes in-contact-with-a-surface, $h_{2x} = h_{2z}$ was assigned a fixed value of $295 \text{ W/m}^2\text{C}$.

Data from Tables 4 and 5 were used in order to obtain simple equations that can be industrially applied to assess the effects of the external temperature and h on freezing times of suspended or incontact-with-a-surface cubed yellow potatoes and ullucus (Equations 17–20). The forward stepwise regression method was used to develop polynomial equations in order to predict freezing times to reach -15°C in the warmest points as functions of the external temperature in the equipment ($T_m, ^\circ\text{C}$) and the heat transfer coefficient ($h_{1x} = h_{1y} = h_{1z}, \text{ W/m}^2\text{C}$). Good values of coefficients of determination (R^2) were observed between the freezing times estimated by FDM proposed and the freezing times estimated by polynomial equations.

FIGURE 2

(a) Experimental and predicted temperature history during freezing process of suspended cubed yellow potatoes ($2 \times 2 \times 2$ cm) using finite difference scheme proposed. (b) Determination of $h_{1x} = h_{1y} = h_{1z}$ for suspended cubed yellow potatoes by optimization of RMSE. (c) Position of thermocouples (central, blue points, and external point, red points) during freezing process of suspended cubed yellow potatoes

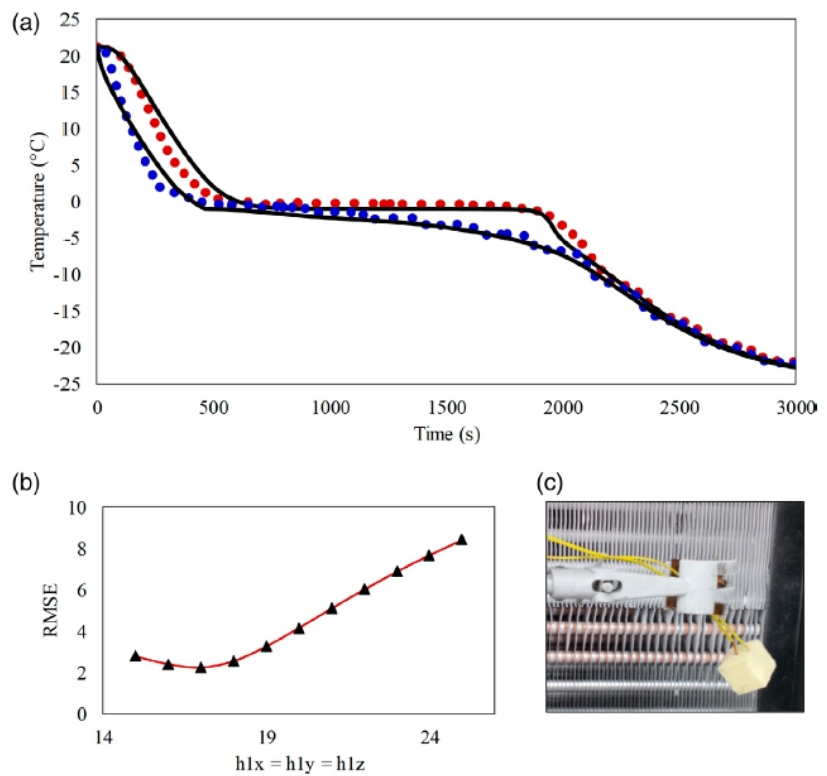


FIGURE 3

(a) Experimental and predicted temperature history during freezing process of suspended (red points) and incontact-with-a-surface cubed ullucus (blue points) ($1.5 \times 1.5 \times 1.5$ cm) using finite difference scheme proposed. (b) Determination of $h_{1x} = h_{1y} = h_{1z}$ for suspended cubed ullucus by optimization of RMSE. (c) Determination of $h_{1x} = h_{1y} = h_{1z}$ and $h_{2x} = h_{2z}$ for incontact-with-a-surface cubed ullucus by optimization of the minimum value of RMSE

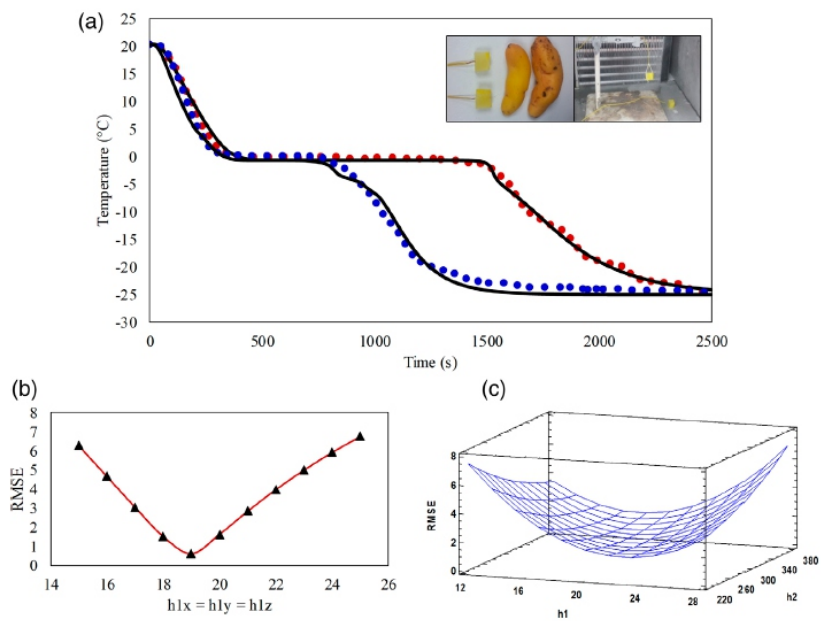


TABLE 3 Thermophysical properties potato, ullucu, and agar gel

Thermophysical properties	Potato	Ullucu	Agar-agar ^a
Bound water factor	0.18	0.18	-
Unfreezable water (%)	2.10	4.88	-
Initial freezing temperature (°C)	-0.98	-0.67	0.00
ρ unfrozen (kg/m ³)	1,160.58	1,053.49	997.10
ρ frozen (kg/m ³)	1,083.55	987.70	919.60
k unfrozen (W/m°C)	0.57	0.56	0.58
k frozen (W/m°C)	2.22	2.09	2.45
c_p unfrozen (J/kg°C)	3,445.73	3,770.98	4,180.00
c_p frozen (J/kg°C)	1,835.48	2,092.84	1,913.00

^aThermal properties of water.

For suspended cubed potatoes, $-40^\circ\text{C} \leq T_m \leq -25^\circ\text{C}$, and $15 \leq h \leq 30 \text{ W/m}^2\text{C}$.

$$F_t (\text{min}) = 156.73 - 4.511(h_1) + 3.522(T_m) + 0.05083(h_1)^2 + 0.02950(T_m)^2 - 0.03441(h_1 T_m), \quad (17)$$

with $R^2 = 0.9981$.

For in-contact-with-a-surface cubed potatoes, $-40^\circ\text{C} \leq T_m \leq -25^\circ\text{C}$, and $15 \leq h \leq 30 \text{ W/m}^2\text{C}$.

$$F_t (\text{min}) = 86.36 - 1.673(h_1) + 2.222(T_m) + 0.01650(h_1)^2 + 0.01992(T_m)^2 - 0.01544(h_1 T_m), \quad (18)$$

TABLE 4 Effects of heat transfer coefficients $h_{1x} = h_{1y} = h_{1z}$ (W/m²C) and external temperatures (T_m) on freezing times (min) of cubed yellow potatoes suspended and in-contact-with-a-surface ($2 \times 2 \times 2$ cm), considering $T_i = 20^\circ\text{C}$ and a final temperature of -15°C

Cube of yellow potato suspended				
T_m (°C)	$h_{1x} = h_{1y} = h_{1z}$ (W/m ² C)			
	15	20	25	30
-25	44.42 min	33.9 min	27.55 min	23.35 min
-30	36.68	27.98	22.8	19.25
-40	27.32	20.88	16.93	14.28
Cube of yellow potato in-contact-with-a-surface				
T_m (°C)	$h_{1x} = h_{1y} = h_{1z}$ (W/m ² C)			
	15	20	25	30
-25	28.12 min	23.8 min	21.27 min	19.55 min
-30	22.92	19.95	17.97	16.32
-40	17.23	14.82	13.63	12.25

with $R^2 = 0.9969$.

For suspended cubed ullucus, $-40^\circ\text{C} \leq T_m \leq -25^\circ\text{C}$, and $15 \leq h \leq 30 \text{ W/m}^2\text{C}$.

$$F_t (\text{min}) = 127.70 - 3.660(h_1) + 2.995(T_m) + 0.041(h_1)^2 + 0.02567(T_m)^2 - 0.02915(h_1 T_m), \quad (19)$$

with $R^2 = 0.9979$.

TABLE 5 Effects of heat transfer coefficients $h_{1x} = h_{1y} = h_{1z}$ (W/m²C) and external temperatures (T_m) on freezing times of cubed ullucus suspended and in-contact-with-a-surface ($1.5 \times 1.5 \times 1.5$ cm) considering $T_i = 20^\circ\text{C}$ and a final temperature of -15°C

Cube of ullucu suspended				
T_m (°C)	$h_{1x} = h_{1y} = h_{1z}$ (W/m ² C)			
	15	20	25	30
-25	34.65 min	26.2 min	21.17 min	17.82 min
-30	28.2	21.33	17.23	14.52
-40	20.67	15.63	12.63	10.65
Cube of ullucu in-contact-with-a-surface				
T_m (°C)	$h_{1x} = h_{1y} = h_{1z}$ (W/m ² C)			
	15	20	25	30
-25	19.93 min	17.6 min	15.35 min	13.83 min
-30	16.38	14.1	12.62	11.45
-40	12.27	10.63	9.53	8.78

For in-contact-with-a-surface cubed ullucus, $-40^\circ\text{C} \leq T_m \leq -25^\circ\text{C}$, and $15 \leq h \leq 30 \text{ W/m}^2\text{C}$.


$$F_t (\text{min}) = 65.65 - 1.1136(h_1) + 1.879(T_m) + 0.00939(h_1)^2 + 0.01833(T_m)^2 - 0.01164(h_1 T_m), \quad (20)$$


with $R^2 = 0.9992$.

4 | CONCLUSIONS

A mathematical model was developed to simulate the heat transfer during the freezing process of 3D cubes using the FDM. The proposed algorithm used the composition of the food to determine the thermophysical properties of potatoes and ullucus, which were included in the computer program written in Visual Basic language. The mathematical model was developed to simulate the heat transfer during the freezing process of suspended and in-contact-with-a-surface cubes. The numerical solution was validated using cubes of yellow potatoes, ullucus, and agar gel, which were frozen suspended and in-contact-with-a-surface. The experimental data showed the need to include, in the numerical solution, a pseudo convective coefficient (294.9–370.7 W/m²°C) in order to simulate the heat transfer during freezing process of cubic particles in-contact-with-a-surface. A good agreement was found between experimental and simulated temperatures using the model developed (RMSE < 2°C). The numerical model developed can be applied to simulate the freezing process of other tubers and thus it can help in the optimization and control of the process.

ORCID

Walter Salas-Valerio 
<https://orcid.org/0000-0002-4143-4003>

Julio Vidaurre-Ruiz 
<https://orcid.org/0000-0003-0980-9474>

REFERENCES

REFERENCES

Association of Official Analytical Chemists. (2000). Official methods of analysis (17th ed.). Gaithersburg, MD: Author.

Boonsupthip, W., & Heldman, D. R. (2007). Prediction of frozen food properties during freezing using product composition. *Journal of Food Science*, 72(5), 254–263. <https://doi.org/10.1111/j.1750-3841.2007.00364.x>

Boonsupthip, W., Sajjaanantakul, T., & Heldman, D. R. (2009). Use of average molecular weights for product categories to predict freezing characteristics of foods. *Journal of Food Science*, 74(8), E417–E425. <https://doi.org/10.1111/j.1750-3841.2009.01309.x>

Campos, D., Chirinos, R., Gálvez Ranilla, L., & Pedreschi, R. (2018). Bioactive potential of Andean fruits, seeds, and tubers. *Advances in Food and Nutrition Research*, 84, 287–343. <https://doi.org/10.1016/bs.afnr.2017.12.005>

Campos, D., Noratto, G., Chirinos, R., Arbizu, C., Roca, W., & CisnerosZevallos, L. (2006). Antioxidant capacity and secondary metabolites in four species of Andean tuber crops: Native potato (*Solanum* sp.),

mashua (*Tropaeolum tuberosum* Ruiz & Pavón), Oca (*Oxalis tuberosa* Molina) and ulluco (*Ullucus tuberosus* Caldas). *Journal of the Science of Food and Agriculture*, 86(10), 1481–1488. <https://doi.org/10.1002/jsfa.2529>

Choi, Y., & Okos, M. (1986). Effects of temperature and composition on the thermal properties of foods. In M. Le Maguer & P. Jelen (Eds.), *Food engineering and process applications*, Vol. 1, Transport phenomena (pp. 93–101). London: Elsevier Applied Science.

Cleland, A. C., & Earle, R. L. (1977). A comparison of analytical and numerical methods of predicting the freezing times of foods. *Journal of Food Science*, 42(5), 1390–1395. <https://doi.org/10.1111/j.1365-2621.1977.tb14506.x>

Cleland, A. C., & Earle, R. L. (1979). A comparison of methods for predicting the freezing times of cylindrical and spherical foodstuffs. *Journal of Food Science*, 44(4), 958–963. <https://doi.org/10.1111/j.1365-2621.1979.tb03422.x>

Cleland, D. J., Cleland, A. C., & Earle, R. L. (1987). Prediction of freezing and thawing times for multi-dimensional shapes by numerical methods. *International Journal of Refrigeration*, 10(4), 234–240. [https://doi.org/10.1016/0140-7007\(87\)90058-2](https://doi.org/10.1016/0140-7007(87)90058-2)

Cornejo, I., Cornejo, G., Ramírez, C., Almonacid, S., & Simpson, R. (2016). Inverse method for the simultaneous estimation of the thermophysical properties of foods at freezing temperatures. *Journal of Food Engineering*, 191, 37–47. <https://doi.org/10.1016/j.jfoodeng.2016.07.003>

Delgado, A. E., & Sun, D. (2001). Heat and mass transfer models for predicting freezing processes—A review. *Journal of Food Engineering*, 47(3), 157–174. [https://doi.org/10.1016/S0260-8774\(00\)00112-6](https://doi.org/10.1016/S0260-8774(00)00112-6)

Dima, J. B., Santos, M. V., Baron, P. J., Califano, A., & Zaritzky, N. E. (2014). Experimental study and numerical modeling of the freezing process of marine products. *Food and Bioproducts Processing*, 92(1), 54–66. <https://doi.org/10.1016/j.fbp.2013.07.012>

Ebrahimnia-Bajestan, E., Niazmand, H., Ehteminan-Farooji, V., & Ebrahimnia, E. (2012). Numerical modeling of the freezing of a porous humid food inside a cavity due to natural convection. *Numerical Heat Transfer; Part A: Applications*, 62(3), 250–269. <https://doi.org/10.1080/10407782.2012.691050>

Ferreira, S. R. (2017). Temps de congélation d'une plaque par la méthode des lignes. *International Journal of Refrigeration*, 75, 77–94. <https://doi.org/10.1016/j.ijrefrig.2017.01.007>

Ferreira, S. R., Rojas, L. O. A., Souza, D. F. S., & Oliveira, J. A. (2016). Temps de congélation d'un cylindre infini et d'une sphère en utilisant la méthode des lignes. *International Journal of Refrigeration*, 68, 37–49. <https://doi.org/10.1016/j.ijrefrig.2016.01.021>

- Fricke, B. A., & Becker, B. R. (2006). Sensitivity of freezing time estimation methods to heat transfer coefficient error. *Applied Thermal Engineering*, 26(4), 350–362. <https://doi.org/10.1016/j.applthermaleng.2005.07.005>
- James, C., Purnell, G., & James, S. J. (2015). A review of novel and innovative food freezing technologies. *Food and Bioprocess Technology*, 8(8), 1616–1634. <https://doi.org/10.1007/s11947-015-1542-8>
- Loeffen, M. P. F., Earle, R. L., & Cleland, A. C. (1981). Two simple methods for predicting food freezing times with time-variable boundary conditions. *Journal of Food Science*, 46(4), 1032–1034. <https://doi.org/10.1111/j.1365-2621.1981.tb02986.x>
- López-Leiva, M., & Hallström, B. (2003). The original Plank equation and its use in the development of food freezing rate predictions. *Journal of Food Engineering*, 58(3), 267–275. [https://doi.org/10.1016/S02608774\(02\)00385-0](https://doi.org/10.1016/S02608774(02)00385-0)
- Mannapperuma, J. D., & Singh, R. P. (1988). Prediction of freezing and thawing times of foods using a numerical method based on enthalpy formulation. *Journal of Food Science*, 53(2), 626–630. <https://doi.org/10.1111/j.1365-2621.1988.tb07770.x>
- Meade, B., Baldwin, K., & Calvin, L. (2010). Peru: An emerging exporter of fruits and vegetables. Report from the Economic Research Service, No. FTS-345-01, Washington, D.C: United States Department of Agriculture. Retrieved from https://www.ers.usda.gov/webdocs/publications/37036/8042_fts34501.pdf?v=4.
- Norton, T., Delgado, A., Hogan, E., Grace, P., & Sun, D. W. (2009). Simulation of high pressure freezing processes by enthalpy method. *Journal of Food Engineering*, 91(2), 260–268. <https://doi.org/10.1016/j.foodeng.2008.08.031>
- Pham, Q. T. (1985). A fast, unconditionally stable finite-difference scheme for heat conduction with phase change, 28(11), 2079–2084.
- Pham, Q. T. (2006). Modelling heat and mass transfer in frozen foods: A review. *International Journal of Refrigeration*, 29(6), 876–888. <https://doi.org/10.1016/j.ijrefrig.2006.01.013>
- Rahman, M. S., Machado-Velasco, K., Sosa-Morales, M., & Velez-Ruiz, J. F. (2009). Freezing point: Measurement, data, and prediction. In M. S. Rahman (Ed.), *Food properties handbook* (2nd ed., p. 838). Boca Raton, FL: Taylor & Francis Group, LLC.
- Saad, Z., & Scott, E. P. (1997). Analysis of accuracy in the numerical simulation of the freezing process in food materials. *Journal of Food Engineering*, 31(1), 95–111. [https://doi.org/10.1016/S0260-8774\(96\)00029-5](https://doi.org/10.1016/S0260-8774(96)00029-5)
- Schwartzberg, H. G. (1976). Effective heat capacities for the freezing and thawing of food. *Journal of Food Science*, 41(1), 152–156. <https://doi.org/10.1111/j.1365-2621.1976.tb01123.x>
- Schwartzberg, H. G. (1977). Effective heat capacities for the freezing and thawing of foods. *Freezing, Frozen Storage and Freeze-Drying* (pp.303– 310). Paris: International Institute of Refrigeration.
- Tocci, A. M., & Mascheroni, R. H. (1995). Numerical models for the simulation of the simultaneous heat and mass transfer during food freezing and storage. *International Communications in Heat and Mass Transfer*, 22(2), 251–260. [https://doi.org/10.1016/0735-1933\(95\)00010-0](https://doi.org/10.1016/0735-1933(95)00010-0)
- Vidaurre-Ruiz, J. M., & Salas-Valerio, W. F. (2017). Modeling heat transfer during blanching of cubic particles of Loche (Cucurbita moschata Duch.) and potato (*Solanum tuberosum* L.) using finite difference method. *Journal of Food Process Engineering*, 40(3), e12451. <https://doi.org/10.1111/jfpe.12451>
- Wang, Z., Wu, H., Zhao, G., Liao, X., Chen, F., Wu, J., & Hu, X. (2007). One-dimensional finite-difference modeling on temperature history and freezing time of individual food. *Journal of Food Engineering*, 79(2), 502–510. <https://doi.org/10.1016/j.foodeng.2006.02.012>
- Wu, X. F., Zhang, M., Adhikari, B., & Sun, J. (2017). Recent developments in novel freezing and thawing technologies applied to foods. *Critical Reviews in Food Science and Nutrition*, 57(17), 3620–3631. <https://doi.org/10.1080/10408398.2015.1132670>
- Xu, J. C., Zhang, M., Mujumdar, A. S., & Adhikari, B. (2017). Recent developments in smart freezing technology applied to fresh foods. *Critical Reviews in Food Science and Nutrition*, 57(13), 2835–2843. <https://doi.org/10.1080/10408398.2015.1074158>
- Zhao, Y., & Takhar, P. S. (2017). Freezing of foods: Mathematical and experimental aspects. *Food Engineering Reviews*, 9(1), 1–12. <https://doi.org/10.1007/s12393-016-9157-z>

How to cite this article: Salas-Valerio W, Solano-Cornejo M, Zelada-Bazán M, Vidaurre-Ruiz J. Three-dimensional modeling of heat transfer during freezing of suspended and in-contact-with-a-surface yellow potatoes and ullucus. *J Food Process Eng*. 2019;e13174. <https://doi.org/10.1111/jfpe.13174>